Appl. Phys. A (2016) 122:408
DOI 10.1007/s00339-016-9757-8

Applied Physics A
Materials Science & Processing

Heat conductivity of copper in two-temperature state

K. P. Migdal[1] · Yu. V. Petrov[2,3] · D. K. Il'nitsky[1] · V. V. Zhakhovsky[1,4] · N. A. Inogamov[1,2] · K. V. Khishchenko[4] · D. V. Knyazev[3,4,5] · P. R. Levashov[4,6]

Received: 18 October 2015 / Accepted: 12 February 2016

Abstract Electron–ion relaxation lasts few tens of picoseconds in a submicrometer surface layer of metal after irradiation by femtosecond laser pulse of moderate intensity. During this stage, the electron temperature is many times higher than ion (lattice) temperature. The rate of this relaxation is slower for noble metals due to their small electron–ion coupling. Thus, effects caused by high electron temperature reveal more obviously for those metals. To study electron transport in noble metal nanofilms, we combine the first-principle calculations and our analytical models. The newly calculated electron–phonon coupling and heat conductivity are used in two-temperature hydrodynamics modeling. Results of such modeling are in good agreement with the experimental data and molecular dynamics simulation.

✉ K. P. Migdal
migdal@vniia.ru

[1] Centre of Fundamental and Applied Research, Dukhov Research Institute of Automatics (VNIIA), Moscow, Russian Federation

[2] Landau Institute for Theoretical Physics, Russian Academy of Science, Moscow, Russian Federation

[3] Moscow Institute of Physics and Technology, Moscow, Russian Federation

[4] Joint Institute of High Temperatures, Moscow, Russian Federation

[5] State Scientific Center of the Russian Federation, Institute for Theoretical and Experimental Physics, National Research Centre Kurchatov Institute, Moscow, Russian Federation

[6] Tomsk State University, Tomsk, Russian Federation

1 Introduction

The importance of electron–ion (e-i) relaxation is in its role in the formation of electron and ion pressures which may generate shocks and rarefaction waves. According to the two-temperature model (TTM) [1], three parameters of irradiated matter in addition to electron pressure [electron heat capacity, electron heat conductivity, and electron–phonon (e–ph) coupling] are responsible for the behavior of heated metal surface during the e-i relaxation.

In the work [2] with 70-nm copper nanofilm, a quantitative agreement between experimental XAS data and TTM modeling of e-i relaxation was obtained. Also, the equivalence of electron structures for solid and liquid phases of copper was shown but only for temperatures much lower than the Fermi temperature. In the TTM modeling [2], only one term responsible for e–ph heat transfer was taken into account, which is the most simple choice for TTM modeling. On the other hand, as was shown in the work [3], the consideration of e–ph heat transfer is necessary even for modeling of processes with temperatures about 1 kK.

Among the aforementioned parameters of TTM, only heat conductivity depends on density ρ, electron, and ion temperatures (T_e and T_i). While electron heat capacity, electron pressure, or e–ph coupling (by the model [4]) can be found using DFT calculation for a single atom in ideal lattice, the heat conductivity is determined by the use of quantum molecular dynamics (QMD) and Kubo-Greenwood theory. To this date, some results for aluminum [5–7], copper [8], and gold [9] were obtained. The growth of heat conductivity with T_e in the range of 10–100 kK predicted in those works is in contradiction with the phenomenological models [10, 11].

Published online: 16 March 2016

Here, we present the results of copper heat conductivity calculation by Kubo-Greenwood approach on the basis of quantum molecular dynamics modeling. The obtained data were used for TTM modeling of e-i relaxation in copper nanofoil after irradiation with the parameters defined in [2]. Using the approach for calculation of e–ph coupling given in [12, 13], we also considered such mechanisms of heat transfer or loss as heat conductivity and work of hydrodynamic forces caused by pressure gradient.

2 Computational details

Calculation of copper e–ph coupling has been performed according to the two-parabolic model for two-band metals [12]. To use this model, it is necessary to obtain the partial electron densities of states for valence bands, which can be represented as $g_i = n_i\sqrt{\varepsilon - \varepsilon_i}(\delta\varepsilon_i)^{-1.5}$, where n_i, ε_i, and $\delta\varepsilon_i$ are concentration of electrons, minimum of energy, and bandwidth for a band with index i, respectively. These characteristics of a valence band have been found using density functional theory (DFT) and VASP package [14, 15]. We used for DFT calculations PAW representation of planewave basis, energy cutoff 500 eV, $21 \times 21 \times 21$ Monkhorst-Pack grid, and 20 empty levels per atom.

As it was revealed in [16], the calculated density of states (DoS) for noble metals changes notably if T_e grows from 0.3 kK to a few tens kK. We can also consider only $4s^1$ and $3d^{10}$ electronic bands because the next band $3p^6$ lies significantly lower than these bands. According to our DFT calculations, the gap between $3p6$ and $4s1$ bands is equal to $\sim$60 eV and is almost independent from such thermodynamical parameters as ρ, T_e and T_i. The changes in DoS caused by compression are also noticeable if we consider the hydrostatic compressions corresponding to pressures up to 100 GPa (see upper part of Fig. 1).

The results of DFT calculation of copper DoS were used to fit n_i, ε_i, and $\delta\varepsilon_i$ as functions of ρ and T_e. We considered that such basic electron structure properties as bandwidths and gaps between bands and the Fermi energy do not depend on copper phase state. We can see in Fig. 1 that effect of phase state is negligible at low T_e. At higher $T_e = 55$ kK and ion temperature $T_i = 2$ kK, DoS for liquid copper is slightly shifted to the Fermi energy. As it will shown hereafter, the maximal T_e in our TTM modeling are limited by $\sim$55 kK, so we can neglect the difference discussed here. These data were used to carry out calculation on the basis of the formulae (8–9) presented in [12].

To calculate heat conductivity using QMD, we firstly need to obtain a thermodynamic state with fixed density, ion, and electron temperatures in a supercell, as it is described in [5–7, 9]. Initially, all atoms with perfect lattice

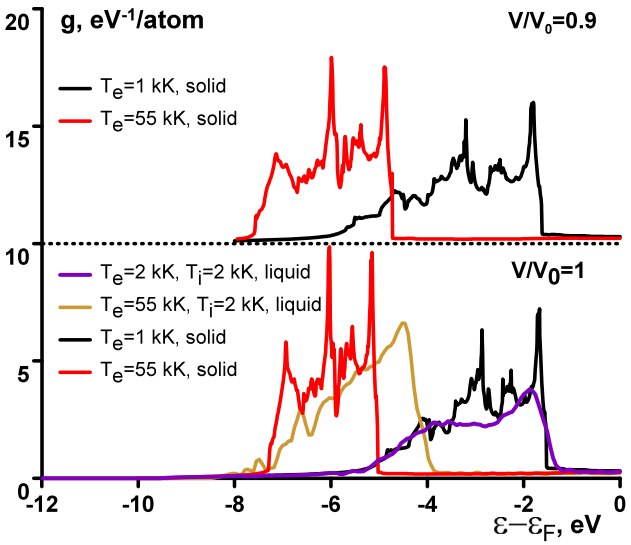

Fig. 1 Density of states for copper at the equilibrium volume (at the *bottom*) and hydrostatic compression to $V/V_0 = 0.9$ (at the *top*). For comparison, the densities of states for liquid copper at the same ρ and T_e are shown for $V/V_0 = 1$

sites are placed into the cubic supercell with a size of a few lattice parameters. The isochoric heating and melting are produced by a thermostat until a target ion temperature is established. Then, some ion configurations are selected for a next stage where electron wave functions will be determined in DFT calculation. This stage is necessary to obtain momentum matrix elements which are used in Kubo-Greenwood formula at the final stage [7]. During two last steps, the effect of ion temperature is implicit because the ion positions found by QMD depend on this temperature. Positions of ions can be characterized by a radial distribution function (RDF). Comparison between RDF and experimental data provided in [6] shows that the ion distribution can be reproduced by using of such small supercells. Electron temperature is fixed during all these calculations at the level defined by Fermi–Dirac smearing. In our work, we follow the scheme described above.

ion configurations for copper in liquid state were obtained from QMD performed by the VASP. The computational cell has 32 atoms. A final ion temperature was achieved by the Nose–Hoover thermostat. After heating, the cell was relaxing in NVE ensemble during 0.5–1 ps to forget the work of thermostat. Other parameters used in this calculation were energy cutoff 300 eV, only Γ-point in Brillouin zone, and 15 empty electron levels per atom.

Electron heat conductivity of liquid copper was calculated employing the Kubo-Greenwood theory by using the full-electron and pseudopotential approaches. We applied four different configurations from QMD stage to obtain necessary statistics for each considered thermodynamic state. Full-electron calculation has been carried out with

the help of FP-LAPW code Elk [18]. In this case, the local density approximation (LDA) for xc-functional was used. For pseudopotential calculation, the planewave code VASP was applied.

Performing FP-LAPW calculations, we found following conditions of convergence: at T_e up to 7.5 kK, we used $8 \times 8 \times 8$ Monkhorst-Pack grid, and 11 empty electron levels per an atom. At higher T_e, Monkhorst-Pack grid was simplified to $4 \times 4 \times 4$, but number of empty electron levels per atom increased to 20. The multiplication of muffin-tin radius on maximum electron wave number was set to 7. Interpolating the tabular data, we have obtained the fittings for heat conductivity in the ranges of ρ, T_i and T_e under consideration. For example, an expression used to fit FP-LAPW data for heat conductivity is

$$\kappa_{FE} = \gamma_0 \frac{\beta_i(\rho/\rho_0)^b + (T_e/T_0)^g}{\left(C_i + (T_i/T_0)^d\right)(1 + \gamma_m(T_e/T_0)^s)}. \quad (1)$$

where we used $\gamma_0 = 184.3\,\mathrm{W/(K\,m)}$, $\beta_i = 0.799, b = 0.895, T_0 = 11.605\,\mathrm{kK}, \rho_0 = 8\,\mathrm{g/cc}, g = 2.239, C_i = 1.215, d = 2.035, \gamma_m = 0.005, s = 3.24$.

The modeling by methods of TTM and classical molecular dynamics (MD) was performed for the experimental conditions [2] with using the new data presented here. EAM interatomic potential [19] is utilized. Hot electrons in MD modeling were reproduced by Monte Carlo particles [20]. In TTM modeling, the presented here results for heat conductivity and e–ph coupling were used to resolve the system of 2THD equations. Cold energy and ion contribution used with our data for heated electron thermodynamics are taken from a semiempirical EoS for copper in e-i equilibrium [21]. To compare correctly our results with the experimental data in [2], the calculated electron temperatures at different times were averaged with mass attenuation coefficient [22].

3 Results

The results of e–ph coupling calculation with the two-parabolic model parameters depended on density and electron temperature are shown in Fig. 2. According to the represented data, e–ph coupling α of copper increases with ρ significantly in our model. On the other hand, the growth of α due to increasing of T_e from 1 up to 40 kK is moderate and weaker than one predicted by Lin et al. [4]. We consider this difference between our and Lin et al.'s results as a consequence of electron d-band shift to lower energies which was not taken into account in [4] (see Fig. 1). In [24], we have presented results of e–ph coupling calculations where the shift of d-band was taken into account, but the number of d-electrons was fixed. Due to the results

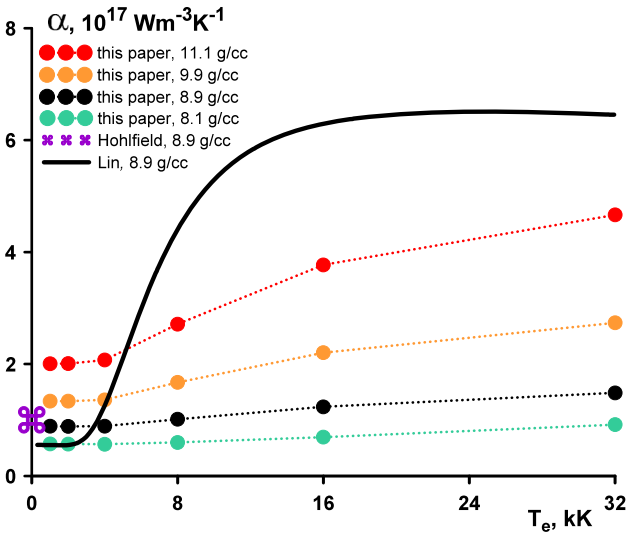

Fig. 2 Electron–phonon coupling of copper as a function of T_e at different densities in comparison with Lin's et al. [4] data. The experimental point at room temperature from [17]

Table 1 *Ab initio* results for heat conductivity of copper

ρ	T_e	T_i	κ_{FE}	$\delta\kappa_{FE}$	κ_{VL}	κ_{VP}	$\delta\kappa_V$
9.4	2	2	139	25	75	86	18
9.4	55	2	3970	30	3980	3970	18
9.4	55	7.5	2150	28	3130	3100	19
8	2	2	124	28	86	86	19
8	7.5	2	174	23.5	224	226	20
8	7.5	7.5	185	24	231	231	19
8	30	2	1230	24	1600	1570	20
8	30	7.5	940	27	1350	1314	18
8	55	2	2920	37	3780	3730	21
8	55	7.5	2160	31	2950	2900	18
7.6	2	2	114	25	85	85	19
7.6	55	2	2490	25	3210	3570	19
7.6	55	7.5	2030	29	2800	2740	19

Here, ρ is density in g/cc, T_e, T_i—electron and ion temperatures in kK, $\kappa_{FE}, \kappa_{VL}, \kappa_{VP}, \delta\kappa_{FE}, \delta\kappa_V$—heat conductivities in W/(m K) and their relative errors in % of liquid copper calculated by Elk and VASP (for LDA and PBE xc-functionals, here relative errors are of the same value)

shown in [24], we can conclude that d-band shifting reduces e–ph coupling in copper. It is worth noting that our result for the $T_e = 1$ kK and equilibrium density is in good agreement with the experimental data provided by Hohlfield et al. [17].

The results of Kubo-Greenwood calculation for heat conductivity κ_e are summarized in Table 1. Using the results of all described above approaches, we can conclude that the effects of all three thermodynamic parameters (T_e, T_i, ρ) are noticeable. We can conclude that the results of

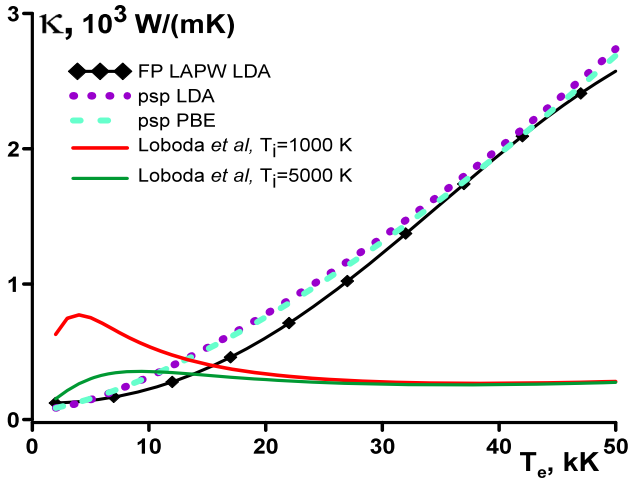

Fig. 3 Heat conductivity of copper obtained by full-electron calculation, pseudopotential calculations using LDA, and PBE xc-functionals as a function of T_e at $\rho = 8$ g/cc and $T_i = 2$ kK. Data for different ion temperatures are from [23]

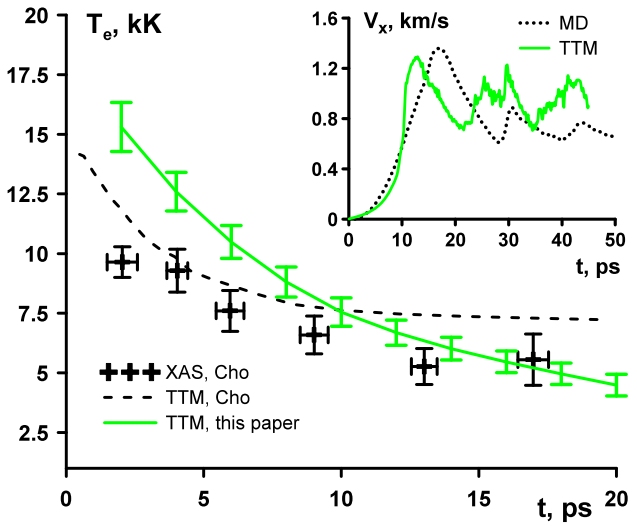

Fig. 4 Relaxation of electron temperature in the copper nanofilm with time. The experimental and TTM modeling results from [2] are compared with our calculations with heat conductivity obtained by the full-electron calculation. In the sidebar, the rear-side surface velocities obtained using MD modeling and TTM modeling are shown

full-electron and pseudopotential calculations are in good agreement. We found that the effect of using PBE xc-functional instead of LDA is negligible due to the data in Table 1. Fittings constructed using functional form of Eq. 1 reproduce the tabular data in Fig. 3 with the relative error 7 %. As it is shown in Fig. 3, the fitted curve predicts the behavior which is similar to presented in [9] for gold. The highest heat conductivity obtained in our calculations corresponds to the highest electron and lowest ion temperatures $T_e = 55$ kK and $T_i = 2$ kK, respectively. Its value of $\sim 3000\,\mathrm{W/(mK)}$ is close to the results of Kubo-Greenwood calculations carried out for aluminum [7] and gold [9].

Figure 4 shows that our approach is in good agreement with experimental points at the final of e-i relaxation. In contrast to the modeling [2], we underline that the hydrodynamic motion was taken into account in our TTM modeling. At the start of e-i relaxation, a greater T_e was obtained because the used e–ph coupling is many times lower than one predicted in [4]. Error bars shown for our calculation correspond to uncertainty of mass attenuation coefficient [22] for the X-ray pulse used in the experiment [2]. The surface velocities of rear sides of films obtained by both TTM and MD modeling are also in good agreement during two-temperature and acoustic stages. Although the peak positions are not coincide, the periods of oscillations (14 ps) caused by acoustic waves in the nanofilm are identical.

4 Discussion and resume

From results obtained for liquid dense copper in two-temperature state, the heat conductivity should be considered as a function of density, electron, and ion temperatures. Using two different approaches for momentum matrix elements calculations, we found these data in good agreement. Also, we obtained e–ph coupling for solid copper which is notably smaller than one provided in [4].

The results of TTM modeling with the newly calculated data for electron thermodynamics and transport properties are in good agreement with experiment [2].

Acknowledgments The research has been performed under financial support from Russian Science Foundation (RSCF) (Project No. 14-19-01599).

References

1. S.I. Anisimov, B.L. Kapeliovich, T.L. Perel'man, Sov. Phys. JETP **39**, 375 (1974)
2. B.I. Cho, K. Engelhorn, A.A. Correa, T. Ogitsu, C.P. Weber, H.J. Lee, J. Feng, P.A. Ni, Y. Ping, A.J. Nelson, D. Prendergast, R.W. Lee, R.W. Falcone, P.A. Heimann, Phys. Rev. Lett. **106**, 167601 (2011)
3. Y. Wang, X. Ruan, A.K. Roy, Phys. Rev. B **85**, 205311 (2012)
4. Z. Lin, L.V. Zhigilei, V. Celli, Phys. Rev. B **77**, 075133 (2008)
5. M.P. Desjarlais, J.D. Kress, L.A. Collins, Phys. Rev. B **66**, 025401 (2002)
6. V. Recoules, J.-P. Crocombette, Phys. Rev. B **72**, 104202 (2005)
7. D.V. Knyazev, P.R. Levashov, Phys. Plasmas **21**, 073302 (2014)
8. J. Clerouin, P. Renaudin, Y. Laudernet, P. Noiret, M.P. Desjarlais, Phys. Rev. B **71**, 064203 (2015)
9. G. Norman, I. Saitov, V. Stegailov, P. Zhilyaev, Contrib. Plasma Phys. **53**, 300 (2013)

10. S.I. Anisimov, B. Rethfeld, Proc. SPIE **3093**, 192 (1997)
11. D. Ivanov, L. Zhigilei, Phys. Rev. B **68**, 066114 (2003)
12. Yu.V. Petrov, N.A. Inogamov, K.P. Migdal, JETP Lett. **97**, 20 (2013)
13. K.P. Migdal, D.K. Il'nitsky, Yu.V. Petrov, N.A. Inogamov, J. Phys. Conf. Ser. **653**, 012086 (2015)
14. G. Kresse, J. Furthmuller, Phys. Rev. B **54**, 11169 (1996)
15. G. Kresse, D. Joubert, Phys. Rev. B **59**, 1758 (1999)
16. V. Recoules, J. Clerouin, G. Zerah, P.M. Anglade, S. Mazevet, Phys. Rev. Lett. **96**, 055503 (2006)
17. J. Hohlfield, S.-S. Wellershoff, J. Gudde, U. Conrad, V. Jahnke, E. Matthias, Chem. Phys. **251**, 237 (2000)
18. Elk is an all-electron full-potential linearised augmented-plane-wave (fp-lapw) code released under either the gnu general public license (gpl) or the gnu lesser general public license (lgpl). elk code is available on http://elk.sourceforge.net
19. R. Perriot, V.V. Zhakhovsky, N.A. Inogamov, I.I. Oleynik, J. Phys. Conf. Ser. **500**, 172008 (2014)
20. N.A. Inogamov, V.V. Zhakhovsky, AYa. Faenov, V.A. Khokhlov, V.V. Shepelev, I.Y. Skobelev, Y. Kato, M. Tanaka, T.A. Pikuz, M. Kishimoto, M. Ishino, M. Nishikino, Y. Fukuda, S.V. Bulanov, T. Kawachi, Yu.V. Petrov, S.I. Anisimov, V.E. Fortov, Appl. Phys. A **101**, 87 (2010)
21. http://www.ihed.ras.ru/rusbank
22. C.T. Chantler, J. Phys. Chem. Ref. Data **24**, 71 (1995)
23. P.A. Loboda, N.A. Smirnov, A.A. Shadrin, N.G. Karlykhanov, High Energy Density Phys. **7**, 361 (2011)
24. K.P. Migdal, Yu.V. Petrov, N.A. Inogamov, Proc. SPIE **9065**, 906503 (2013)